

An unprecedented polyoxometalate-based 1D double chain compound with opposite charges enables conductivity improvement

Ke-Ke Guo, Xin-Ye Jiang, Ming Xu, Feng-Yan Li*, Si-Meng Dong, Yue Zheng and Lin Xu*

Key Laboratory of Polyoxometalate and Reticular Material Chemistry of Ministry of Education, Faculty of Chemistry, Northeast Normal University, Changchun, Jilin 130024, P. R. China.

Corresponding author. E-mail: linxu@nenu.edu.cn, lify525@nenu.edu.cn

Experimental Section

General Materials and Methods

The $K_5[BW_{12}O_{40}] \cdot 11H_2O$ (BW_{12}) was synthesized according to previous literature.¹ Elemental analyses (C, H and N) were measured on a Perkin-Elmer 2400 CHN Elemental Analyzer. All chemical reagents and solvents were available commercially and used as received without further purification. Metal elemental analyses were determined by a Leaman inductively coupled plasma (ICP) spectrometer. Thermogravimetric analysis (TGA) was performed on a PerkinElmer TGA7 thermal analyzer from room temperature at a heating rate of $10\text{ }^\circ\text{C min}^{-1}$ under a continuous stream of N_2 using crushed polycrystalline samples. FT-IR spectra were recorded on an Alpha Centaur FT/IR spectrometer using a KBr pellet in the frequency range of $4000\text{-}400\text{ cm}^{-1}$. Powder X-ray diffraction (PXRD) patterns were recorded using Cu $K\alpha$ radiation ($\lambda = 1.54056\text{ \AA}$) in the range $2\theta = 5\text{-}50^\circ$ at 293 K on a Philips X'Pert-MPD instrument. The UV-vis diffuse reflectance spectra (DRS) of compound **1** was measured on a Cary7000 UV-Vis-NIR Spectrophotometer from 200 to 800 nm at room temperature to reveal both the optical absorption properties and the optical band gap (E_g), which can be defined as the intersection point between the energy axis and

the line extrapolated from the linear portion of the adsorption edge in a plot of Kubelka-Munk function F against E . The $F = (1 - R)^2/2R$, was transformed from the recorded diffuse reflectance data, in which R is the reflectance of an infinitely thick layer at a given wavelength.² A barium sulfate (BaSO_4) pellet was used as the standard with 100% reflectance. The local coordination geometries and symmetries of all Cu^{II} ions were analyzed by Continuous Shape Measure (CShM) calculation using SHAPE 2.0 software.^{3,4}

The photoelectrochemical (PEC) sensing experiments were carried out by using a CHI 660 Electrochemical Workstation (Shanghai Chenhua Instrument Corp. China) at room temperature. A three-electrode system was employed in a quartz cell with a saturated calomel electrode (SCE) as the reference electrode, a Pt wire as the counter electrode, and the composite film-assembled FTO glass as the working electrode. The illumination area of working electrodes was set constant at $1.0 \times 1.0 \text{ cm}^2$. The photocurrent experiments were carried out at a constant bias of 0.6 V under light irradiation conditions ($\lambda > 420 \text{ nm}$, 300 W Xenon arc lamp, PLS-SXE300C/300CUV, $100 \text{ mW} \cdot \text{cm}^{-2}$) upon on-off cycling irradiation with xenon light (intervals of 30 s) under different H_2O_2 concentrations. Mott-Schottky plots were obtained by measuring Impedance-Potential curves at the fixed frequency of 500 and 1000 Hz, respectively. An aqueous solution of 0.5 M Na_2SO_4 (pH = 5.8) that was exposed to air was used as electrolyte throughout the experiments. The obtained potential (vs. SCE) was converted to E_{RHE} (E_{NHE} at pH = 0) by the equation $E_{\text{RHE}} = E_{\text{SCE}} + 0.0592\text{pH} + 0.241$.⁵

Synthesis of $\{\text{BW}_{12}\text{O}_{40}[\text{Cu}(2,2'\text{-bipy})_2]_2[\text{Cu}(2,2'\text{-bipy})(\text{H}_2\text{O})]\}\{\text{BW}_{12}\text{O}_{40}[\text{Cu}(2,2'\text{-bipy})_2][\text{Cu}(2,2'\text{-bipy})(\text{H}_2\text{O})_2]\} \cdot 7\text{H}_2\text{O}$ (1).

A mixture of BW_{12} (0.018 mmol, 0.060 g), 2,2'-bipy (0.1 mmol, 0.0156 g), $\text{Cu}(\text{NO}_3)_2 \cdot 3\text{H}_2\text{O}$ (0.2 mmol, 0.048 g) was dissolved in 8 mL of distilled water at room temperature. The pH value was adjusted to 2.0 by 2 M HCl and the mixture was stirred for 30 min. The resulting mixture was transferred into a 25 mL Teflon-lined stainless steel autoclave and kept at 160 °C for 72 h. After slow cooling to room temperature, dark blue block-like crystals were obtained. Yield: ca. 48% (based on

W). Anal. Calcd (%) for $C_{80}H_{84}B_2Cu_5N_{16}O_{94}W_{24}$: C, 12.77; H, 1.13; N, 2.98; Cu, 4.22; B, 0.29; W, 58.62. Found: C, 13.09; H, 1.15; N, 3.12; Cu, 4.26; B, 0.32; W, 58.73. IR (KBr pellet, cm^{-1}): 3128 (w), 1602 (s), 1401 (s), 1162 (w), 955(s), 911 (s), 823 (s), 528 (w).

X-ray Crystallography.

All the data were collected with a Bruker Apex CCD diffractometer using Mo-K α radiation ($\lambda=0.71073$ Å) at 298.15 K. The structures were solved by direct methods and was refined by full-matrix least-squares methods with a suite of SHELX programs via Olex2 interface.⁶⁻⁹ Non-hydrogen atoms were refined anisotropically. The hydrogen atoms bonded to some lattice water molecules were not discernible from the last final difference Fourier maps and consequently were not included in the structure refinement. Other hydrogen atoms were placed in calculated positions and refined by using a riding model. Pertinent crystal data and relevant refinement parameters for compound **1** are listed in Table S4. The CCDC data can be obtained free of charge from The Cambridge Crystallographic Data Centre via www.ccdc.cam.ac.uk/data_request/cif. CCDC nos. 2080632.

Conductivity Measurements

The procedures for preparing pellets and measuring their I - V curves are described in the experimental section. The electrical conductivity (σ) of the material was then calculated by the following equation.

$$\sigma = l/(RA)$$

where R is the electrical resistance, l is the thickness of the pellet, and A is the cross-section area of the pellet.¹⁰ The average value of electrical conductivity for each material was calculated from three pellet measurements (Table S3).

Table S1. Continuous Shape Measures calculation for the Cu^{2+} ions in chain 1 and chain 2.

Cu1 in chain 1	PP-5	D_{5h}	Pentagon	30.579
	vOC-5	C_{4v}	Vacant octahedron	1.409
	TBPY-5	D_{3h}	Trigonal bipyramid	4.833
	SPY-5	C_{4v}	Spherical square pyramid	1.160

	JTBPY-5	D_{3h}	Johnson trigonal bipyramid J12	7.968
Cu4 in chain 2	HP-6	D_{6h}	Hexagon	29.839
	PPY-6	C_{5v}	Pentagonal pyramid	24.457
	OC-6	Oh	Octahedron	3.138

Table S2. The bond-valence sum (BVS) calculations of W for compound **1**.

Compound 1					
Atom	Oxidation states	Atom	Oxidation states	Atom	Oxidation states
W1	6.15	W2	6.10	W3	6.12
W4	6.18	W5	6.17	W6	5.95
W7	6.32	W8	6.20	W9	6.12
W10	6.38	W11	6.11	W12	6.08
W13	6.13	W14	6.17	W15	5.98
W16	6.30	W17	6.10	W18	6.01
W19	6.31	W20	6.22	W21	6.30
W22	6.13	W23	6.06	W24	6.27

Table S3. The average value of electrical conductivity for compound **1** and BW_{12} .

	number of times	1/R (S)	A (cm ²)	l (mm)	σ (S cm ⁻¹)	average σ (S cm ⁻¹)
Compound 1	1	1.8×10^{-8}	0.785	0.500	1.14×10^{-9}	1.17×10^{-9}
	2	2.1×10^{-8}	0.785	0.423	1.13×10^{-9}	
	3	2.5×10^{-8}	0.785	0.393	1.25×10^{-9}	
BW_{12}	1	3.2×10^{-10}	0.785	0.312	1.27×10^{-11}	1.26×10^{-11}
	2	2.4×10^{-10}	0.785	0.386	1.18×10^{-11}	
	3	2.2×10^{-10}	0.785	0.485	1.35×10^{-11}	

Table S4. Crystal data and structure refinement parameters for compound **1**.

Compound	1
----------	----------

Empirical formula	$C_{80}H_{84}B_2Cu_5N_{16}O_{94}W_{24}$
Formula weight	7525.08
Temperature/K	296.15
Crystal system	monoclinic
Space group	$P2_1/c$
$a/\text{\AA}$	26.620(10)
$b/\text{\AA}$	22.211(8)
$c/\text{\AA}$	26.964(9)
$\alpha/^\circ$	90
$\beta/^\circ$	117.198(6)
$\gamma/^\circ$	90
Volume/ \AA^3	14180(9)
Z	4
$\rho_{\text{calc}} \text{ g/cm}^3$	3.458
μ/mm^{-1}	20.209
$F(000)$	13124.0
Reflections collected	65531
Independent reflections	24507
R_{int}	0.0891
Data/restraints/parameters	24507/3608/1921
Goodness-of-fit on F^2	1.042
Final R indexes	$R_1 = 0.0623$
$[I \geq 2\sigma(I)]$	$wR_2 = 0.1149$
Final R indexes	$R_1 = 0.1008$
[all data]	$wR_2 = 0.1319$

Table S5. Comparisons of the sensing performances of different H_2O_2 sensors.

POMs	Coexisting Substances	Methods	Linear range (μM)	LOD (μM)	Ref.
$[\text{PMo}_{12}\text{O}_{40}]^{3-}$	rGO	EC	2000-20000	67.9	11
$[\text{PMo}_{12}\text{O}_{40}]^{3-}$	PPy	EC	200-30000	50	12
NENU5	-	EC	1000-5000	1.3	13
$\{\text{AsW}_{12}\text{O}_{40}\}$	-	EC	1.43-1890	0.48	14
$[\text{P}_2\text{Mo}_{18}\text{O}_{62}]^{3-}$	OMC	EC	1.13-6250	0.377	15
$[\text{CoCoW}_{11}\text{O}_{39}]^8$	TiO_2	EC	2-280	0.8	16
-	-	-	-	-	-
$[\text{EuW}_{10}\text{O}_{36}]^{9-}$	Chitosan	Fluorescence	1.1-66	0.11	17
TiO_2	-	PEC	0.5-35	0.18	18
BiVO_4	-	PEC	50-1500	8.5	19
CuO	-	PEC	100-1000	180	20
CdS	-	PEC	25-1000	19	21
CuO/ZnO	-	PEC	1.99-17540	0.44	22

EC: electrochemical; PEC: photoelectrochemical; rGO: reduced grapheme oxide; PPy: Polypyrrole; OMC: ordered mesoporous carbon; NENU5: $[\text{Cu}_2(\text{BTC})_{4/3}(\text{H}_2\text{O})_2]_6[\text{H}_3\text{PMo}_{12}\text{O}_{40}]$ (BTC = Trimesic acid); $\{\text{AsW}_{12}\text{O}_{40}\}$: $[(\text{Ag}_7\text{bpy}_7\text{Cl}_2)\{\text{AsW}_2^{\text{V}}\text{W}_{10}^{\text{VI}}\text{O}_{40}\}] \cdot \text{H}_2\text{O}$ (bpy = 4,4'-bipyridyl).

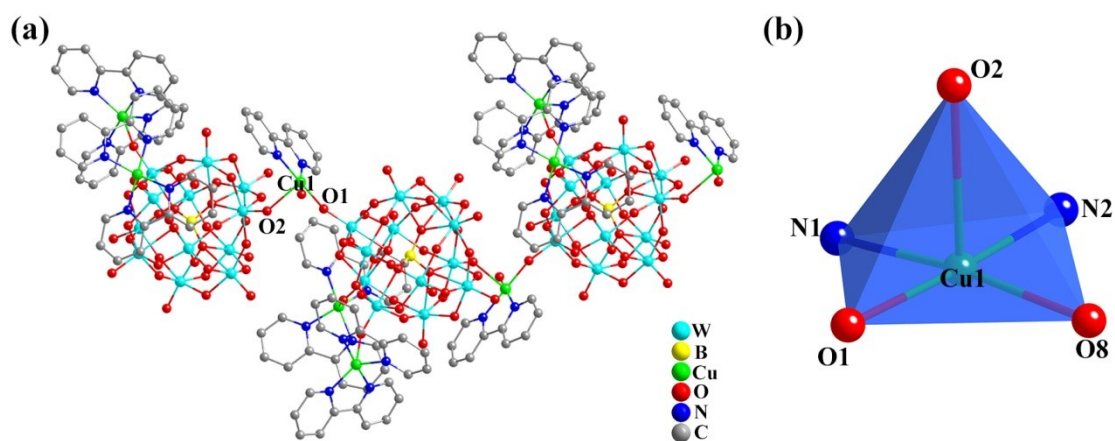


Fig. S1. The chain 1 of compound 1 (a); the coordination geometry of Cu1(b).

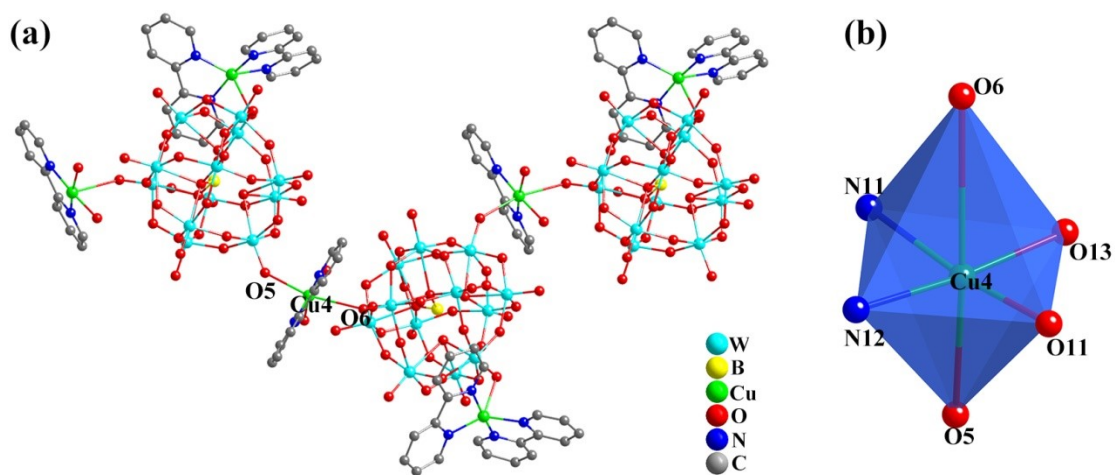


Fig. S2. The chain 2 of compound 1 (a); the coordination geometry of Cu4(b).

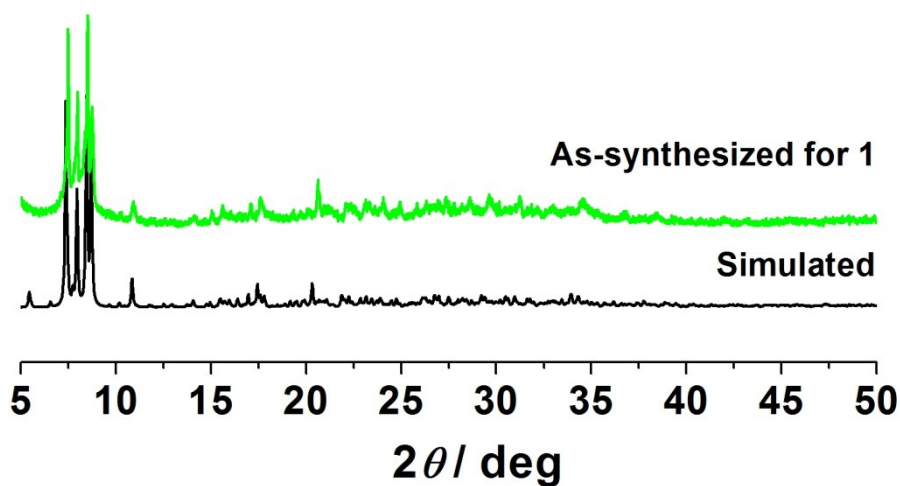


Fig. S3. PXRD patterns of as-synthesized samples of compound **1** and its simulated patterns.

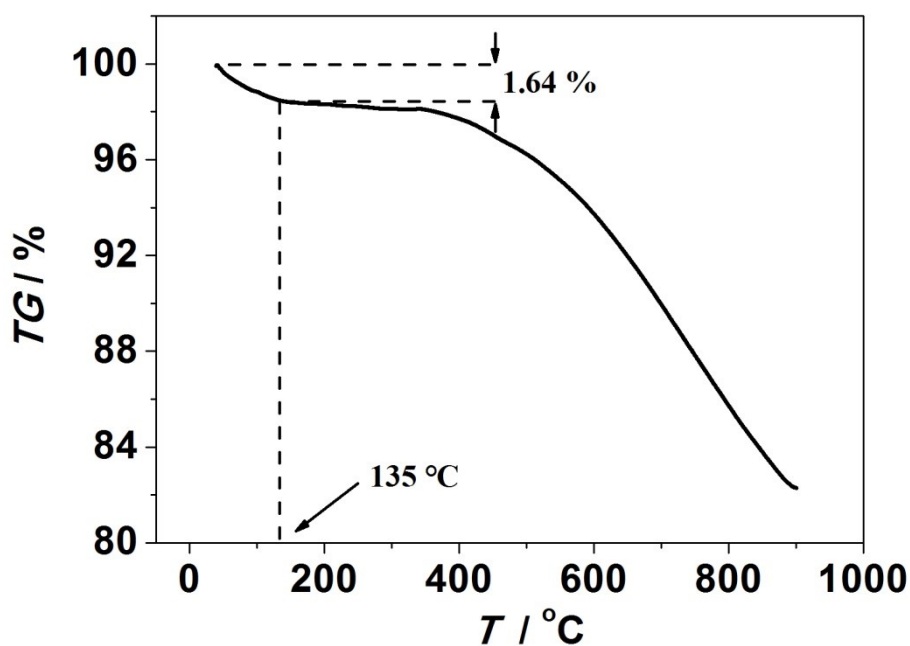


Fig. S4. TGA curve of compound **1**.

The thermogravimetric analysis (TGA) of compound **1** (Fig. S4) shows that it went through a weight loss of 1.64% in the temperature range of 25–135 °C, corresponding to the weight loss of seven free lattice H₂O molecules (calc. 1.67%); this result is consistent with the content of H in free lattice water by elemental analysis. Then, its framework kept stable until approximately 345 °C. After that, its framework started to collapse with a series of complicated weight losses.

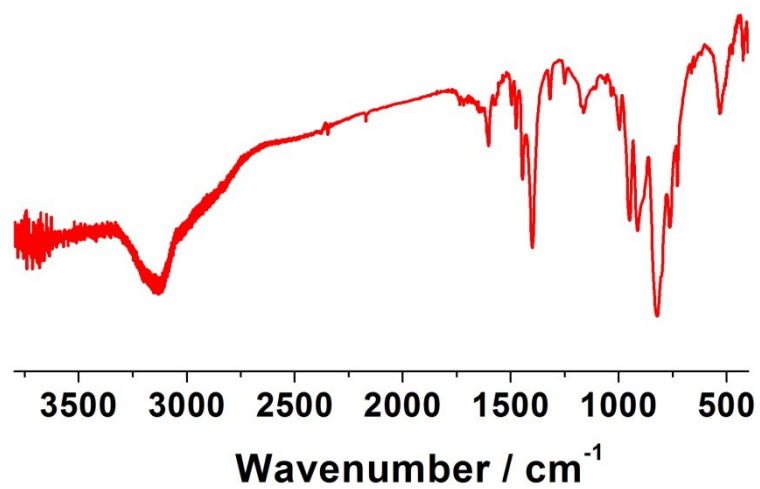


Fig. S5. IR spectra of compound 1.

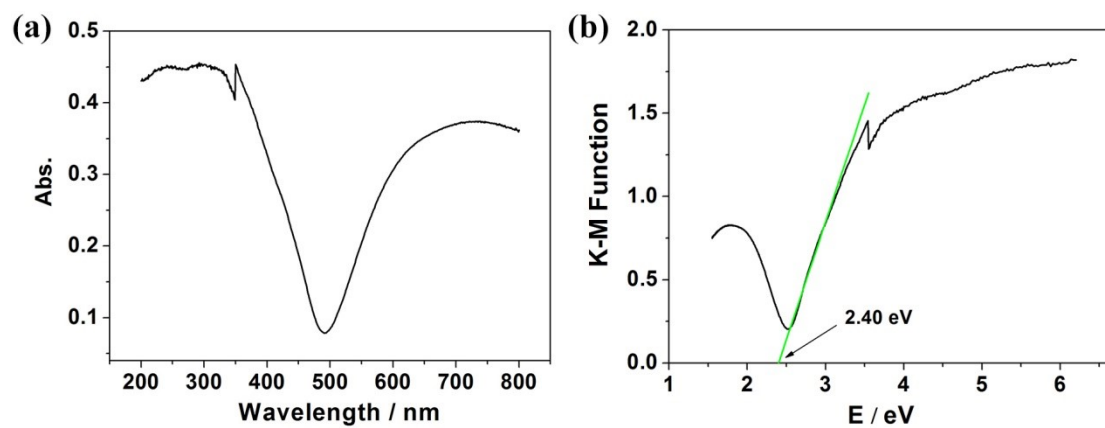


Fig. S6. UV-vis diffuse reflectance spectra of compound 1 (a); diffuse reflectance UV-vis-NIR spectra of K-M functions versus energy (eV) of compound 1 (b).

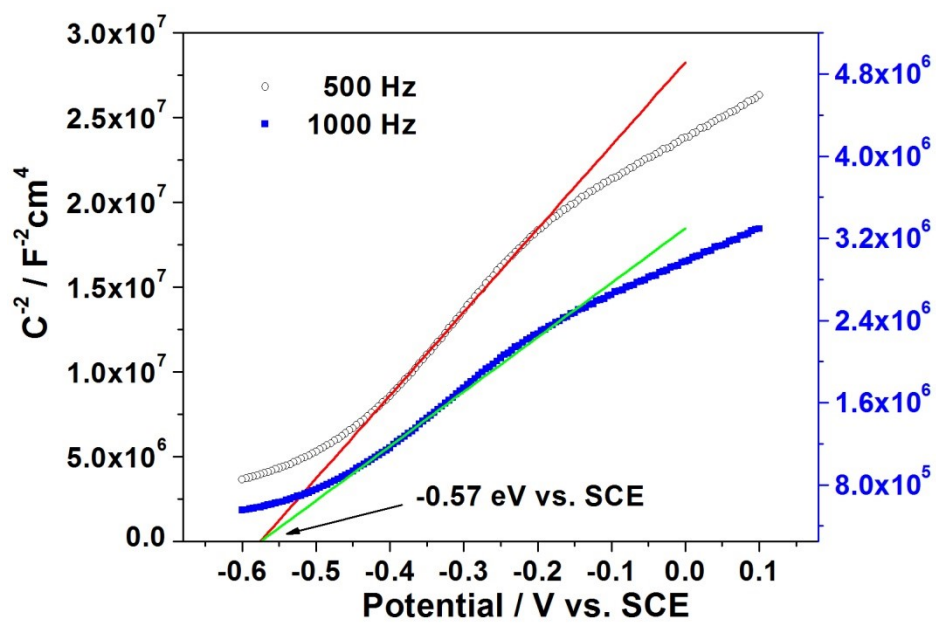


Fig. S7. Mott-Schottky plots of compound 1.

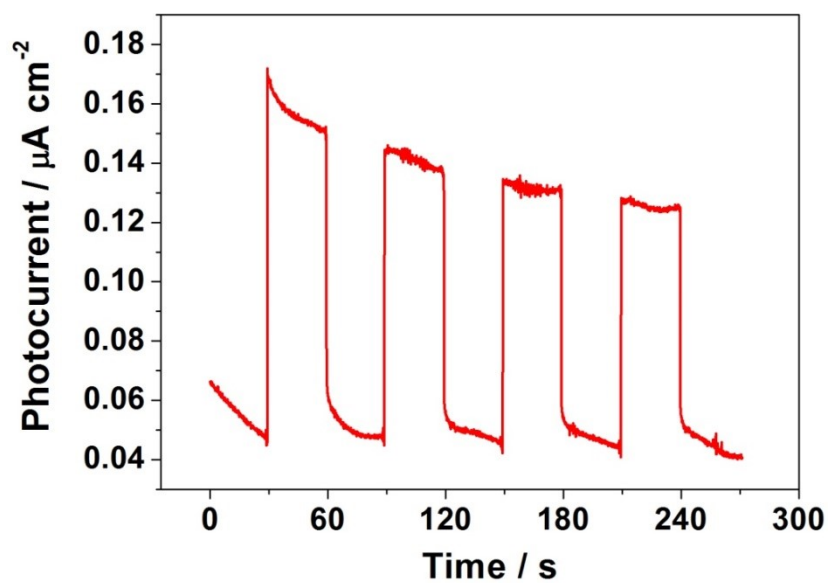


Fig. S8. The transient photocurrent responses of compound 1.

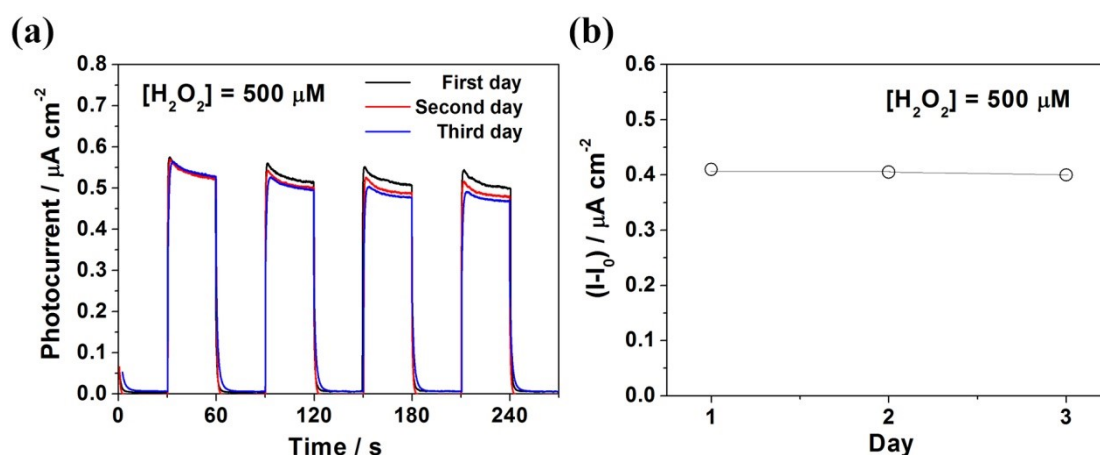


Fig. S9. Photocurrent responses at 500 μM H_2O_2 using compound **1** electrode at different days (a); Output photo response measured with the same compound **1** photoanode for the PEC sensing of 500 μM H_2O_2 performed three days apart (b).

References

- 1 R. D. Claude, F. Michel, F. Raymonde, T. René, *Inorg. Chem.*, 1983, **22**, 207-216.
- 2 L. Liu, J. Ding, M. Li, X. Lv, J. Wu, H. Hou, Y. Fan, *Dalton Trans.*, 2014, **43**, 12790-12799.
- 3 H. Zabrodsky, S. Peleg, D. Avnir, *J. Am. Chem. Soc.*, 1992, **114**, 7843-7851.
- 4 M. Pinsky, D. Avnir, *Inorg. Chem.*, 1998, **37**, 5575-5582.
- 5 W. C. Fang, R. Tao, Z. B. Jin, Z. X. Sun, F. Y. Li, L. Xu, *J. Alloy. Compd.* 2019, **797**, 140-147.
- 6 G. M. Sheldrick, SHELX-2014, University of Göttingen, Göttingen, 2014.
- 7 G. M. Sheldrick, *Acta Crystallogr.*, 2015, **C71**, 3-8.
- 8 O. V. Dolomanov, L. J. Bourhis, R. J. Gildea, J. A. K. Howard and H. Puschmann, *J. Appl. Crystallogr.*, 2009, **42**, 339-341.
- 9 L. J. Bourhis, O.V. Dolomanov, R. J. Gildea, J. A. K. Howard and H. Puschmann, *Acta Crystallogr.*, 2015, **A71**, 59-75.
- 10 Y. C. Chen, W. H. Chiang, D. Kurniawan, P. C. Yeh, K. I. Otake, C. W. Kung, *ACS Appl. Mater. Interfaces.*, 2019, **11**, 35319-35326.
- 11 M. H. Yang, D. S. Kim, T. J. Lee, S. J. Lee, K.G. Lee and B. G. Choi, *J. Colloid. Interf. Sci.*, 2016, **468**, 51-56.

- 12 X. Wang, H. Zhang, E. Wang, Z. Han and C. Hua, *Mater. Lett.*, 2004, **58**, 1661-1664.
- 13 C. Wang, M. Zhou, Y. Ma, H. Tan, Y. Wang and Y. Li, *Chem. Asian J.*, 2018, **13**, 2054-2059.
- 14 L. Cui, K. Yu, J. Lv, C. Guo and B. Zhou, *J. Mater. Chem. A.*, 2020, **8**, 22918-22928.
- 15 M. Zhou, L. P. Guo, F. Y. Lin and H. X. Liu, *Anal. Chim. Acta.*, 2007, **587**, 124.
- 16 Y. Li, W. Bu, L. Wu and C. Sun, *Sens. Actuators, B.*, 2005, **107**, 921.
- 17 J. Lu, Q. Kang, J. Xiao, T. Wang, M. Fang and L. Yu, *Carbohydr. Polym.*, 2018, **200**, 560-566.
- 18 D. Chen, H. Zhang, X. Li, J. Li, *Anal. Chem.*, 2010, **82**, 2253-2261.
- 19 Z. Yu, S. Lv, R. Ren, G. Cai, D. Tang, *Microchim. Acta.*, 2017, **184**, 799-806.
- 20 M. Rehosek, D. Mitoraj, M. Bledowski, R. Beranek, *Electroanal.*, 2016, **28**, 2327-2334.
- 21 Z. Yue, W. Zhang, C. Wang, G. Liu, W. Niu, *Mater. Lett.*, 2012, **74**, 180-182.
- 22 H. Wu, H. Y. Chung, D. C. W. Tsang, N. M. Huang, Z. Xie, H. N. Lim, Y. S. Ok, Y. H. Ng, *Chem. Eng. Sci.*, 2020, **226**, 115886.